

Anatomy of a Simple Acyl Intermediate in Enzyme Catalysis: Combined Biophysical and Modeling Studies on Ornithine Acetyl Transferase

Aman Iqbal,[†] Ian J. Clifton,[†] Maria Bagonis,[‡] Nadia J. Kershaw,[†] Carmen Domene,[‡]
Timothy D. W. Claridge,[†] Christopher W. Wharton,[§] and Christopher J. Schofield^{*,†}

*Chemistry Research Laboratory, University of Oxford, 12 Mansfield Road,
Oxford, OX1 3TA, U.K., Physical and Theoretical Chemistry Laboratory, Department of
Chemistry, University of Oxford, Oxford, OX1 3QZ, U.K., School of Biosciences, University of
Birmingham, Edgbaston, Birmingham, B15 2TT, U.K.*

Received September 18, 2008; E-mail: christopher.schofield@chem.ox.ac.uk

Abstract: Acyl-enzyme complexes are intermediates in reactions catalyzed by many hydrolases and related enzymes which employ nucleophilic catalysis. However, most of the reported structural data on acyl-enzyme complexes has been acquired under noncatalytic conditions. Recent IR analyses have indicated that some acyl-enzyme complexes may be more flexible than most crystallographic analyses have implied. OAT2 is a member of the N-terminal nucleophile (Ntn) hydrolase enzyme superfamily and catalyzes the reversible transfer of an acetyl group between the α -amino groups of ornithine and glutamate in a mechanism proposed to involve an acyl-enzyme complex. We have carried out biophysical analyses on ornithine acetyl transferase (OAT2), both in solution and in the crystalline state. Mass spectrometric studies identified Thr-181 as the residue acetylated during OAT2 catalysis; ¹³C NMR analyses implied the presence of an acyl-enzyme complex in solution. Crystallization of OAT2 in the presence of *N*- α -acetyl-L-glutamate led to a structure in which Thr-181 was acetylated; the carbonyl oxygen of the acyl-enzyme complex was located in an oxyanion hole and positioned to hydrogen bond with the backbone amide NH of Gly-112 and the alcohol of Thr-111. While the crystallographic analyses revealed only one structure, IR spectroscopy demonstrated the presence of two distinct acyl-enzyme complex structures with carbonyl stretching frequencies at 1691 and 1701 cm⁻¹. Modeling studies implied two possible acyl-enzyme complex structures, one of which correlates with that observed in the crystal structure and with the 1691 cm⁻¹ IR absorption. The second acyl-enzyme complex structure, which has only a single oxyanion hole hydrogen bond, is proposed to give rise to the 1701 cm⁻¹ IR absorption. The two acyl-enzyme complex structures can interconvert by movement of the Thr-111 side-chain alcohol hydrogen away from the oxyanion hole to hydrogen bond with the backbone carbonyl of the acylated residue, Thr-181. Overall, the results reveal that acyl-enzyme complex structures may be more dynamic than previously thought and support the use of a comprehensive biophysical and modeling approach in studying such intermediates.

Introduction

Proteases and related enzymes that employ a nucleophilic serine/threonine/cysteine residue (nucleophilic enzymes) that form ester or thioester intermediates during catalysis are among the most studied of all enzymes. Many nucleophilic enzymes have important biomedical roles and are targets for therapeutic intervention via inhibition with small molecules (for reviews see, e.g., refs 1–4). Pioneering studies in mechanistic enzymology, beginning with the serine proteases (such as α -chymotrypsin and trypsin), demonstrated the existence of a covalent

ester or acyl-enzyme complex.^{5–8} Residues important in the requisite general acid base catalysis, both for the formation of the acyl-enzyme complex (including activation of the nucleophilic serine side-chain) and hydrolysis (activation of the water affecting the hydrolysis) steps, have been identified for many nucleophilic enzymes (e.g., refs 1, 9, and 10). For the nucleophilic enzymes that are proteases, a histidine residue commonly acts as a general acid/base, often in conjunction with an adjacent aspartate residue that, together with the nucleophilic residue, forms a ‘catalytic triad’.¹⁰ Structural analyses have revealed that one very well conserved feature of nucleophilic enzymes, and indeed many other enzymes that catalyze reactions involving

[†] Chemistry Research Laboratory, University of Oxford.

[‡] Physical and Theoretical Chemistry Laboratory, University of Oxford.

[§] University of Birmingham.

(1) Hedstrom, L. *Chem. Rev.* **2002**, *102*, 4501–4524.

(2) Turk, B.; Turk, V.; Turk, D. *Biol. Chem.* **1997**, *378*, 141–150.

(3) Artymiuk, P. J. *Nat. Struct. Biol.* **1995**, *2*, 1035–37.

(4) Brannigan, J. A.; Dodson, G.; Duggleby, H. J.; Moody, P. C. E.; Smith, J. L.; Tomchick, D. R.; Murzin, A. G. *Nature* **1995**, *378*, 416–419.

(5) Matthews, B. W.; Sigler, P. B.; Henderson, R.; Blow, D. M. *Nature* **1967**, *214*, 652–656.

(6) Wright, C. S.; Alden, R. A.; Kraut, J. *Nature* **1969**, *221*, 235–42.

(7) Freer, S. T.; Kraut, J.; Robertus, J. D.; Wright, H. T.; Xuong, N. H. *Biochemistry* **1970**, *9*, 1997–2009.

(8) Henderson, R. *J. Mol. Biol.* **1970**, *54*, 341–54.

(9) Hedstrom, L. *Curr. Protoc. Prot. Sci.* **2002**, *21*, 21–10.

(10) Dodson, G.; Wlodawer, A. *Trends Biochem. Sci.* **1998**, *23*, 347–352.

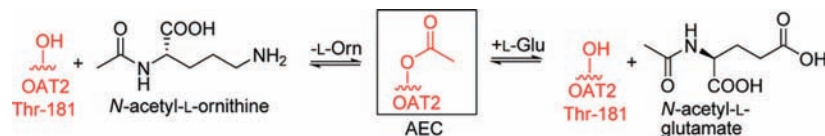


Figure 1. Ornithine acetyl transfer reaction showing the proposed acyl-enzyme complex. The kinetic mechanism is proposed to be ping-pong.⁴⁴

carbonyl groups, is binding of the oxygen of the carbonyl group in an ‘oxyanion hole’. Classically this oxyanion hole involves hydrogen bonding from two main-chain amide NH groups to the two lone pairs of the carbonyl group. Binding in the oxyanion hole serves to polarize the carbonyl group activating it for nucleophilic attack and, with other interactions, to locate the substrate productively in the active site. Crystallographic studies have provided detailed insights into the structures, activation, substrate selectivity, and mechanisms of many nucleophilic enzymes.^{11–15} Many structures of inhibitor complexes have been reported including for compounds that react to form stable acyl-enzyme complexes (see, e.g., refs 16–19). Crystal structures of substrate analogues have also been reported; in the case of proteases, these were initially for nonpeptidic substrate analogues^{20–22} though more recently structures for acyl-enzyme complexes of peptides^{23–30} have been reported. Although these structures have provided extensive structural details and acted as a basis for modeling studies, the nature of crystallographic analyses requires that the population of molecules within each crystal is relatively homogeneous and stable.³¹ Most crystallographic data on acyl-enzyme complexes have been collected either with ‘poor’ substrates/inhibitors, e.g., with a slow hydrolysis rate for the acyl-enzyme complex or by perturbing the catalytic conditions to trap an intermediate (e.g., by mutagenesis or lowering the pH).^{24,26} Thus, there are

questions regarding the relevance of detailed aspects of these structures to those of catalytic intermediates for efficient substrates (Figure 1).

Recent infrared (IR) and modeling studies have implied that the conformations adopted by the carbonyl groups of acyl-enzyme complexes can be more flexible than indicated by crystallographic studies.^{32–34} In the case of one β -lactamase, at least four conformations were observed by IR spectroscopy where only a single acyl-enzyme complex conformation was observed by X-ray analysis.³² X-ray diffraction studies on acyl-enzyme complexes of acylating inhibitors with other β -lactamases have revealed conformations in which the acyl-enzyme complex carbonyl is located both within and outside the oxyanion hole (at least in the crystalline state).^{35–37} These studies have raised the question of whether conformational flexibility is a general feature of acyl-enzyme complexes.

The N-terminal nucleophile (Ntn) enzymes are a ubiquitous superfamily, most of which catalyze hydrolysis or acetyl transfer reactions. The Ntn superfamily includes enzymes with diverse functions including antibiotic hydrolysis,³⁸ plant asparaginase,³⁹ the biosynthesis of purine nucleotides,⁴⁰ glutathione metabolism in bacteria,⁴¹ proteasomal degradation,^{42,43} and many others (for reviews, see refs 3, 4, and 11). Ntn enzymes have a conserved $\alpha\beta\beta\alpha$ fold and are produced as single inactive polypeptides which undergo autocatalysis to produce active heterodimeric forms with the N-terminal nucleophile on the β subunits.

Ornithine acetyl transferases (OATs) are Ntn enzymes that catalyze the reversible transfer of an acetyl group to/from N- α -acetylated (L-ornithine and L-glutamate), via an acyl-enzyme complex.⁴⁴ Because the acyl-enzyme complex of OAT is relatively stable,⁴⁵ its structure is of interest with respect to the

- (11) Oinonen, C.; Rouvinen, J. *Protein Sci.* **2000**, *9*, 2329–2327.
- (12) Wang, Z.; Fast, W.; Valentine, A. M.; Benkovic, S. J. *Curr. Op. Chem. Biol.* **1999**, *3*, 614–622.
- (13) Philippon, A.; Dusart, J.; Joris, B.; Frère, J. M. *Cell. Mol. Life Sci.* **1998**, *54*, 341–346.
- (14) Page, M.; Di Cera, E. *Cell. Mol. Life Sci.* **2008**, *65*, 1220–1236.
- (15) Lowther, W. T.; Matthews, B. W. *Chem. Rev.* **2002**, *102*, 4581–4608.
- (16) Powers, J. C.; Asgjan, J. L.; Ekici, O. D.; James, K. E. *Chem. Rev.* **2002**, *102*, 4639–4750.
- (17) Leung-Toung, R.; Zhao, Y.; Li, W.; Tam, T. F.; Karimian, K.; Spino, M. *Curr. Med. Chem.* **2006**, *13*, 547–581.
- (18) Kisselev, A. F.; Goldberg, A. L. *Chem. Biol.* **2001**, *8*, 739–758.
- (19) Malcolm, G.; Page, P. *Drug Resist. Updates* **2000**, *3*, 109–125.
- (20) Ding, X.; Rasmussen, B. F.; Petsko, G. A.; Ringe, D. *Biochemistry* **1994**, *33*, 9285–9293.
- (21) Dixon, M. M.; Brennan, R. G.; Matthews, B. W. *Int. J. Biol. Macromol.* **1991**, *13*, 89–96.
- (22) Blanchard, H.; James, M. N. G. *J. Mol. Biol.* **1994**, *241*, 574–587.
- (23) Ding, X.; Rasmussen, B. F.; Petsko, G. A.; Ringe, D. *Bioorg. Chem.* **2006**, *34*, 410–423.
- (24) Liu, B.; Schofield, C. J.; Wilmouth, R. C. *J. Biol. Chem.* **2006**, *281*, 24024–24035.
- (25) Wilmouth, R. C.; Clifton, I. J.; Robinson, C. V.; Roach, P. L.; Aplin, R. T.; Westwood, N. J.; Hajdu, J.; Schofield, C. J. *Nat. Struct. Biol.* **1997**, *4*, 456–462.
- (26) Wilmouth, R. C.; Edman, K.; Neutze, R.; Wright, P. A.; Clifton, I. J.; Schneider, T. R.; Schofield, C. J.; Hajdu, J. *Nat. Struct. Biol.* **2001**, *8*, 689–694.
- (27) Katona, G.; Wilmouth, R. C.; Wright, P. A.; Berglund, G. I.; Hajdu, J.; Neutze, R.; Schofield, C. J. *J. Biol. Chem.* **2002**, *277*, 21962–21970.
- (28) Radisky, E. S.; Lee, J. M.; Lu, C. J.; Koshland, D. E. *Proc. Natl. Acad. Sci. U.S.A.* **2006**, *103*, 6835–6840.
- (29) Vivares, D.; Arnoux, P.; Pignol, D. *Proc. Natl. Acad. Sci. U.S.A.* **2005**, *102*, 18848–18853.
- (30) Lee, J.; Feldman, A. R.; Delmas, B.; Paetzel, M. *J. Biol. Chem.* **2007**, *282*, 24928–24937.
- (31) Wilmouth, R. C.; Clifton, I. J.; Neutze, R. *Nat. Prod. Rep.* **2000**, *17*, 527–533.

- (32) Wilkinson, A. S.; Bryant, P. K.; Meroueh, S. O.; Page, M. G.; Mobashery, S.; Wharton, C. W. *Biochemistry* **2003**, *42*, 1950–1957.
- (33) Wilkinson, A. S.; Ward, S.; Kania, M.; Page, M. G.; Wharton, C. W. *Biochemistry* **1999**, *38*, 3851–3856.
- (34) Johal, S. S.; White, A. J.; Wharton, C. W. *Biochem. J.* **1994**, *297*, 281–287.
- (35) Nukaga, M.; Bethel, C. R.; Thomson, J. M.; Hujer, A. M.; Distler, A.; Anderson, V. E.; Knox, J. R.; Bonomo, R. A. *J. Am. Chem. Soc.* **2008**.
- (36) Maveyraud, L.; Mourey, L.; Kotra, L. P.; Pedelacq, J. D.; Guillet, V.; Mobashery, S.; Samama, J. P. *J. Am. Chem. Soc.* **1998**, *120*, 9748–9752.
- (37) Beadle, B. M.; Shoichet, B. K. *Antimicrob. Agents Chemother.* **2002**, *46*, 3978–3980.
- (38) McVey, C. E.; Walsh, M. A.; Dodson, G. G.; Wilson, K. S.; Brannigan, J. A. *J. Mol. Biol.* **2001**, *313*, 139–150.
- (39) Michalska, K.; Bujacz, G.; Jaskolski, M. *J. Mol. Biol.* **2006**, *360*, 105–116.
- (40) Smith, J. L.; Wery, J. P.; Niu, L.; Switzer, R. L.; Zalkin, H.; Satow, Y. *Nature* **1994**, *264*, 1427–33.
- (41) Okada, T.; Suzuki, H.; Wada, K.; Kumagai, H.; Fukuyama, K. *Proc. Natl. Acad. Sci. U.S.A.* **2006**, *103*, 6471–6476.
- (42) Groll, M.; Huber, R. *Biochim. Biophys. Acta* **2004**, *29*, 33–44.
- (43) Seemuller, E.; Lupas, A.; Baumeister, W. *Nature* **1996**, *382*, 468–471.
- (44) Marc, F.; Weigel, P.; Legrain, C.; Almeras, Y.; Santrot, M.; Glansdorff, N.; Sakanyan, Y. *Eur. J. Biochem.* **2000**, *267*, 5217–5226.
- (45) Kershaw, N. J.; McNaughton, H. J.; Hewitson, K. S.; Hernandez, H.; Griffin, J.; Hughes, C.; Greaves, P.; Barton, B.; Robinson, C. V.; Schofield, C. J. *Eur. J. Biochem.* **2002**, *269*, 2052–2059.

question of whether or not acyl-enzyme complexes adopt more than one conformation under catalytic conditions. Here we report a combined biophysical (employing NMR, X-ray, MS, and IR) analysis and modeling approach to the study of the acyl-enzyme complex of OAT2 from *Streptomyces clavuligerus*, an enzyme involved in the biosynthesis of the β -lactamase inhibitor clavulanic acid.⁴⁵ While the X-ray and NMR analyses provided evidence for only a single acyl-enzyme complex structure, IR studies supported by modeling studies revealed two distinct structures for the acyl-enzyme complex.

Experimental Procedures

Protein Expression and Purification. OAT2 was prepared as reported.⁴⁵

Mass Spectrometry. For the MALDI/MS assays, the trypsinolysis experiments comprised purified OAT2 (95 μ M, 8 μ L) and *N*- α -acetyl-L-glutamate (2 mM, 2 μ L) in 50 mM Tris-HCl, pH 7.5 with an incubation time of 2 min. The resultant assay mixture was then separated by SDS-PAGE and trypsin digestion performed as described.⁴⁶ The lyophilized peptide mixtures were then mixed with cyano-4-hydroxycinnamate MALDI matrix (10 mg/mL) in 60% acetonitrile/H₂O/0.1% CF₃CO₂H and spotted directly onto a MALDI target. Samples were analyzed using a MALDI-TOF Micro MX Mass Spectrometer (Waters Micromass). The nondenaturing ESI-MS experiments with intact OAT2/variants used a Micromass BioQ II-ZS triple quadrupole mass spectrometer. For the OAT2-substrate binding experiments, OAT2 (50 μ M) was mixed with *N*- α -acetyl-L-glutamate, in 1:2, 1:5, and 1:10 ratios and injected directly into the mass spectrometer.

Crystallization, Data Collection and Determination of Crystal Structure. Screening for crystallization of OAT2 in the presence of *N*- α -acetyl-L-glutamate used a Cartesian robot at the Oxford Protein Production Facility (OPPF). The optimized crystal growth conditions for 'acyl-OAT2' crystals consisted of OAT2 (12 mg/mL) in ammonium sulfate (1.4 M), lithium sulfate (0.1 M), Tris HCl pH 8.5 (0.1 M), and *N*- α -acetyl-L-glutamate (0.1 M), with incubation at 17 °C. These conditions produced single prism-shaped crystals, of approximate dimensions 0.20 \times 0.15 \times 0.30 mm³, after 7 days (referred to as 'acyl-OAT2' crystals subsequently).

Data were collected using a Bruker MicroStar X-ray generator equipped with a Mar Research Mar345 imaging plate detector. Intensities were integrated and scaled with programs from the HKL2000 suite.⁴⁷ Subsequent data reduction and model refinement used the CCP4 suite.⁴⁸ Four monomers derived from the A chain of wildtype OAT2 (PDB id: 1vz6) were identified using the molecular replacement program PHASER.⁴⁹ The model was refined using REFMAC,⁵⁰ and adjusted using O⁵¹ and COOT.⁵² NCS restraints were applied throughout. The quality and stereochemistry of the structure was monitored after the refinement with WHATCHECK⁵³ and PROCHECK.⁵⁴ For the final refinement, TLS groups were assigned with the TLSMD server.⁵⁵ For other details see Table 1, Supporting Information. Efforts were also undertaken to screen for crystallization at lower pH. However, these efforts resulted in significant protein precipitation (pH < 6). Flash-cooling⁴¹

of these crystals in liquid nitrogen, after serial soaking with *N*- α -acetyl-L-glutamate solutions resulted in structures with only partial occupancy of the substrate in one OAT2 molecule and also scattered, unresolved regions of electron density (data not shown). The PDB code for the acyl-OAT2 structure is 2vzk.

¹³C NMR Spectroscopy. ¹³C NMR experiments were performed using a Bruker AVII 500 spectrometer equipped with a ¹³C-optimized ¹³C{¹H} DUL cryogenic probe regulated at 298 K. *N*- α -Acetyl-L-glutamate labeled with ¹³C at the acetyl carbonyl group was prepared by standard procedures with acetylation of L-glutamate with C-2 ¹³C-labeled acetyl chloride (1 equiv) using triethylamine as the base in aqueous MeOH.

For the observation of an acyl-enzyme complex by NMR, an OAT2 solution was concentrated to 0.9 mM. The reaction mixture consisted of a 10-fold excess of ¹³C-*N*- α -acetyl-L-glutamate, (50 μ L, 9 mM) with OAT2 (500 μ L, in 50 mM Tris-HCl pH 7.5); D₂O (50 μ L) was added for spectrometer field-frequency locking. The reaction time course was monitored at 298 K. For the acetyl transfer experiments, the sample preparations were identical except that equal substrate concentrations of ¹³C-*N*- α -acetyl-L-glutamate and L-ornithine were used. In this case ¹³C NMR spectra were recorded under conditions of high resolution to resolve the *N*- α -acetyl-L-glutamate and *N*- α -acetyl-L-ornithine acetate carbonyl resonances ($\Delta\delta = 2$ Hz).

IR Spectroscopy. For the initial IR experiments, OAT2 (0.75 mM, 0.75 mL) in 50 mM Tris HCl pH 7.5 was lyophilized then resuspended in D₂O and incubated overnight at 4 °C (to reduce the H₂O absorption band) to give a final concentration of 0.5 mM of OAT2. ¹²C-*N*- α -Acetyl-L-glutamate and ¹³C-*N*- α -acetyl-L-glutamate were prepared in 50 mM Tris HCl pH 7.5. Spectra were initially referenced against a D₂O spectrum obtained from 1024 scans. In the reaction mixtures for acyl-enzyme complex observation, a 10-fold excess of *N*- α -acetyl-L-glutamate over OAT2 was used; these solutions comprised OAT2 (100 μ L, 0.75 mM) and ¹²C- or ¹³C-*N*- α -acetyl-L-glutamate (10 μ L, 5 mM) of which 90 μ L was injected into the 'in situ' IR cuvette.³² IR spectra were acquired using a Bruker IFS66 spectrometer; 10 \times 1024 scans were accumulated, with 1 min intervals and a scan rate of 17 s⁻¹ (180 kHz). The OAT2 spectrum was obtained by acquiring 1024 scans of OAT2 (100 μ L, 0.75 mM) diluted with 50 mM Tris HCl (10 μ L, pH 7.5). Model esters (50 mM) were dissolved in D₂O as their hydrochloride salts, with the exception of succinyl-L-phenylalanine methyl ester, which was dissolved in 0.1 M phosphate buffer pH 7.0. The model esters used were δ -*N*-benzoyl-L-Arg ethyl ester, D-Phe methyl ester, *N*-acetyl-L-Lys ethyl ester, Gly-Gly ethyl ester, L-Cys ethyl ester, L-His methyl ester and succinyl-Phe-OMe (all from Sigma, U.K.). The molar integrated absorbance intensities (100 μ m path length) were calculated by band integration and analyzed with curve fitting since in several cases there were two ester carbonyl bands.

Computational Procedures and Molecular Dynamics Simulations. MD calculations were performed on three of the individual OAT2 monomer molecules present in the acyl-OAT2 crystal structure: the AB, CD, and GH molecules {EF (acyl-enzyme) was similar to CD (acyl-enzyme) so was not analyzed}. Residues with missing atoms in the X-ray structures were built using the program psfgen of NAMD2.⁵⁶ The protein complexes were solvated with water and the net charge of each system was neutralized by sodium ions. Water molecules observed in the crystal structures were included in the model. Each system contained between 48 000 and 59 000 atoms. Simulations were performed using NAMD2. The CHARMM27 force field⁵⁷ was used for the protein together with the TIP3 model for water molecules. Parameters were explicitly assigned by identifying molecular fragments already in the

(46) Sleeman, M. C.; Sorensen, J. L.; Batchelar, E. T.; McDonough, M. A.; Schofield, C. J. *J. Biol. Chem.* **2005**, *280*, 34956–34965.

(47) Otwinowski, Z.; Minor, W. *Methods Enzymol.* **1997**, *276*, 307–326.

(48) CCP4 project. *Acta Crystallogr. D* **1994**, *D50*, 760–763.

(49) Read, R. J. *Acta Crystallogr. D* **2001**, *D57*, 1373–1382.

(50) Murshudov, G. N.; Vagin, A. A.; Dodson, E. J. *Acta Crystallogr. D* **1997**, *D53*, 250–255.

(51) Jones, T. A.; Zou, J.-Y.; Cowan, S. W.; Kjeldgaard, M. *Acta Crystallogr. A* **1991**, *A47*, 110–119.

(52) Emsley, P.; Cowtan, K. *Acta Crystallogr. D* **2004**, *D60*, 2126–2132.

(53) Hoof, R. W. W.; Vriend, G.; Sander, C.; Abola, E. E. *Nature* **1996**, *381*, 272.

(54) Laskowski, R. A.; MacArthur, M. W.; Moss, D. S.; Thornton, J. M. *J. Appl. Crystallogr.* **1993**, *26*, 283–291.

(55) Painter, J.; Merritt, E. A. *J. Appl. Crystallogr.* **2006**, *39*, 109–111.

(56) Laxmikant, K.; Robert, S.; Milind, B.; Robert, B.; Attila, G.; Neal, K.; James, P.; Artiomio, S.; Krishnan, V.; Klaus, S. *J. Comput. Phys.* **1999**, *151*, 283–312.

(57) Neria, E.; Fischer, S., a.; Karplus, M. *J. Chem. Phys.* **1996**, *105*, 1902–1921.

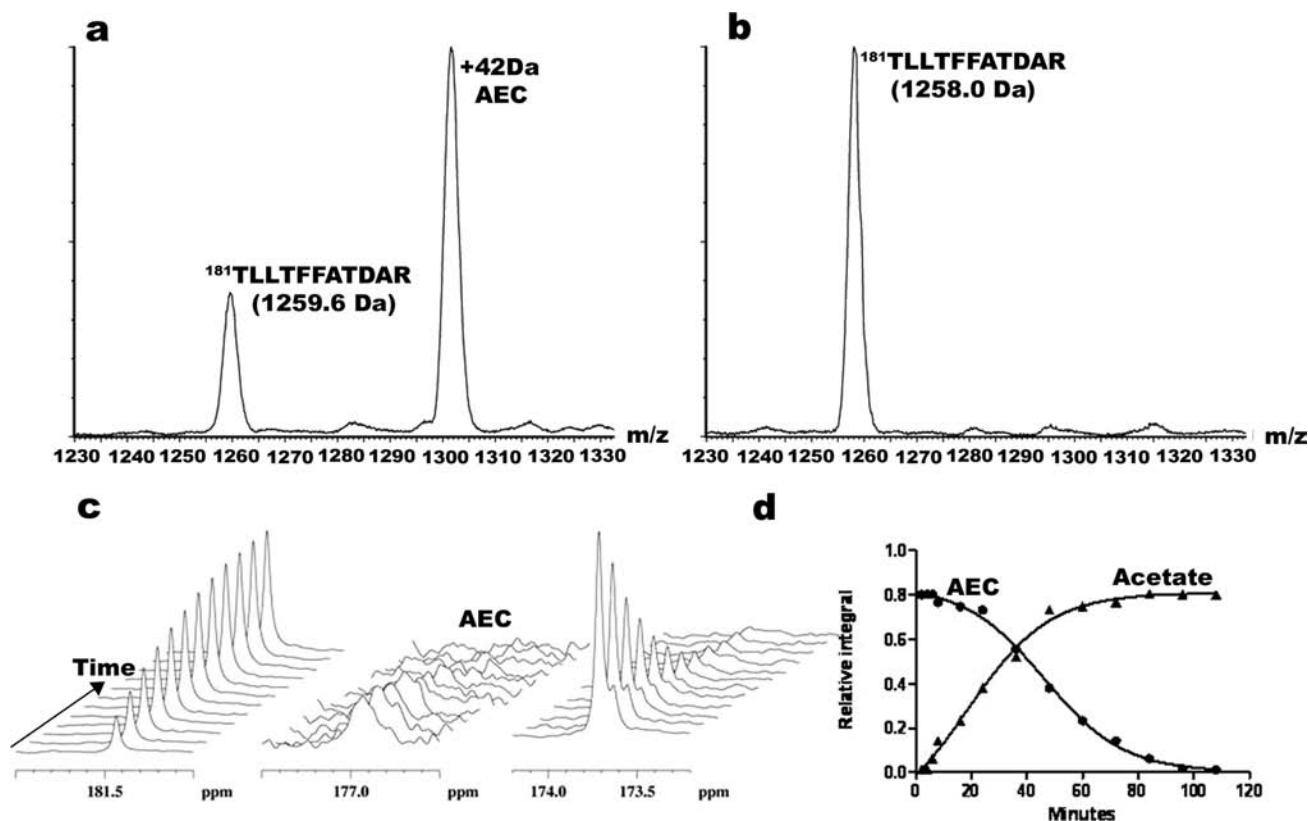


Figure 2. MS and NMR evidence for the acyl enzyme complex (AEC). MS/MS spectra of the $^{181}\text{TLLTFFATDAR}$ peptide from tryptic digestion of OAT2, in the (a) presence of and (b) absence of *N*-acetyl-L-glutamate (*N*- α -acetyl-L-glutamate). Note the +42 Da mass shift in (a) compared to (b). (c) ^{13}C NMR time-course spectra from incubations of OAT2 with *N*- α -acetyl-L-glutamate. The carbonyl group of the assigned acyl-enzyme complex corresponds to the resonance at 176.9 ppm. The other resonances in the spectrum correspond to the substrate carbonyl ^{13}C -*N*- α -acetyl-L-glutamate (174.6 ppm) and product ^{13}C -acetate carbonyl resonance (181.4 ppm). Each time point corresponds to a 6 min increment in incubation time. (d) Kinetics of the hydrolysis of the OAT2 acyl-enzyme complex (as determined by ^{13}C NMR integration and ^{13}C production) (\bullet = acyl-enzyme complex, \blacktriangle = $1\text{-}^{13}\text{C}$ acetate).

CHARMM force field for acetylated Thr181 and the acetate ion. Periodic boundary conditions were adopted and long-range electrostatic interactions were treated by the Particle Mesh Ewald algorithm.⁵⁸ A 12 Å smoothed cutoff was used for the Van der Waals interactions. Smoothing functions were applied to both electrostatic and Van der Waals forces with a switching distance of 2 Å. All the simulations were run in the NPT ensemble. The temperature was maintained at 300 K using the Berendsen thermostat,⁵⁹ and a pressure of 1 atm was maintained using the Nose–Hoover Langevin piston pressure control algorithm.⁶⁰ The time step was set to 1 fs and trajectories were saved every 5 ps. In each case, the system was first energy minimized for 2000 steps using a conjugate gradient procedure and then followed by 4 ns of unconstrained dynamics. Histidines were protonated at the δ position. Except for the *N*-terminal amine of Thr-181, in all the simulations the *N*-terminus and the *C*-terminus were acetylated or amidated, respectively.

Results and Discussion

Mass Spectrometric Analyses of the Acyl-Enzyme Complex.

Initially we used negative ion electrospray ionization mass spectrometry (ESI-MS) under denaturing conditions to verify acetylation of the OAT2 β -subunit. Mixing OAT2 with an excess (20-fold) of either *N*-acetyl-L-glutamate or *N*- α -acetyl-

L-ornithine, resulted in $\sim 20\%$ acetylation of the β -subunit.⁴⁵ Although, *N*- α -acetyl-L-glutamate and *N*- α -acetyl-L-ornithine treatment gave similar levels of acetylation, acetylation with *N*- α -acetyl-L-glutamate occurred more rapidly than with *N*- α -acetyl-L-ornithine (data not shown). In order to investigate whether, as predicted,⁴⁵ Thr-181 is acetylated during catalysis, OAT2 was treated with excess *N*- α -acetyl-L-glutamate and then subjected to trypsinolysis and peptide fragment analysis by MS. A fragment containing Thr-181 ($^{181}\text{TLLTFFATDAR}$) was identified (1259.6 Da) (Figure 2), which had a +42 Da mass increment compared to a control sample not treated with *N*- α -acetyl-L-glutamate indicating that OAT2 forms an acyl-enzyme complex involving Thr-181.

^{13}C NMR Analyses. To demonstrate that OAT2 forms an acyl-enzyme complex in solution we then carried out ^{13}C NMR analyses on an OAT2 solution with *N*- α -acetyl-L-glutamate labeled with ^{13}C at the amide carbonyl (^{13}C -*N*- α -acetyl-L-glutamate). In addition to the sharp resonances observed due to the amide carbonyl group of ^{13}C -*N*- α -acetyl-L-glutamate (174.6 ppm), and the [$2\text{-}^{13}\text{C}$] labeled acetate (181.4 ppm), an additional broad resonance at 176.9 ppm was observed (see Supporting Information, Figure 1). The broad resonance at 176.9 ppm was provisionally assigned as arising from the acyl-enzyme complex because of its shape and chemical shift.⁶¹ The production of acetate is due to the slow hydrolysis of the acyl-enzyme complex in the absence of an acceptor substrate. A

(58) Fang, B.; Martyna, G.; Deng, Y. *Comput. Phys. Commun.* **2007**, *177*, 362–377.

(59) Berendsen, H. J. C.; Postma, J. P. M.; Van Gunsteren, W. F.; Dinola, A.; Haak, J. R. *J. Chem. Phys.* **1984**, *81*, 3684–3690.

(60) Martyna, G. J.; Tobias, D. J.; Klein, M. L. *J. Chem. Phys.* **1994**, *101*, 4177–4189.

(61) Niu, C. H.; Shindo, H.; Cohen, J. S.; Cross, M. *J. Am. Chem. Soc.* **1977**, *99*, 3161–3162.

control experiment with ^{13}C -*N*- α -acetyl-L-glutamate only showed the resonance at 174.7 ppm; an OAT2-only control experiment showed the characteristic protein background, without the resonances at 174.7 and 176.9 ppm (data not shown). The peak at 176.9 ppm was observed at the shortest possible time point of analysis. The rate constant for the acyl-enzyme degradation was $8.7 \times 10^{-3} \text{ s}^{-1}$, and that for acetate production was $8.2 \times 10^{-3} \text{ s}^{-1}$.

To investigate the stability of the acyl-enzyme complex resonance, time-course experiments were then performed on OAT2 and ^{13}C -*N*- α -acetyl-L-glutamate at pH 7.5. A steady reduction in the broad resonance at 176.9 ppm (Figure 2b and c) was observed, together with an increase in acetate resonance (181.4 ppm) coupled to a decrease in the *N*- α -acetyl-L-glutamate resonance (174.6 ppm). It was possible to observe the assigned acyl-enzyme complex resonance at 176.9 ppm for 45 min, after which it was difficult to carry out the integration of the broad acyl-enzyme resonance, as it merged with the baseline (Figure 2b).

To further verify the assignment of the OAT2 acyl-enzyme under our assay conditions, experiments were carried out with α -chymotrypsin and the substrate analogue phenylpropionic acid^{62,63} (Supporting Information, Figure 2) which is known to form an acyl-enzyme complex with α -chymotrypsin. After mixing α -chymotrypsin and imidazole-activated [^{13}C]-phenyl-propionic acid in a 1:10 ratio, an initial ^{13}C NMR analysis showed resonances for substrate and products at 157.5 and 162.9 ppm, respectively (Supporting Information, Figure 2). A broad resonance was observed at 158.5 ppm, very close to the substrate resonance; the resonance at 158.5 ppm was not observed after 10 min of incubation (Supporting Information, Figure 2). This broad resonance was absent in the substrate [^{13}C]-phenyl propionic acid spectrum and was hence assigned as an acyl-enzyme complex (the lower chemical shift value compared to the OAT2 acyl-enzyme complex probably reflects the conjugated nature of phenylpropionic acid).

Crystallographic Analysis of the Acyl-Enzyme Complex.

Following the verification that an acyl-enzyme complex was formed by OAT2 in solution, we then carried out cocrystallization of OAT2 with *N*- α -acetyl-L-glutamate to obtain detailed structural information on the acyl-enzyme complex. The optimization of crystallization conditions led to a 2.1 Å structure ($R_{\text{free}} = 0.26$) of acylated OAT2 (acyl-OAT2).

Preliminary crystallographic work⁶⁴ has shown that OAT2 has the characteristic $\alpha\beta\alpha$ fold of the Ntn enzymes⁴ (Supporting Information, Figure 4). Both in solution and in the crystalline forms, apo-OAT2 (1vz8) and acyl-OAT2 (2vzk) form an $\alpha_4\beta_4$ heterotetramer, with four $\alpha\beta$ monomers per asymmetric unit (Supporting Information, Figure 3). There are thus four $\alpha\beta$ OAT2 monomers and a total of eight subunit chains: A(α), B(β), C(α), D(β), E(α), F(β), G(α), and H(β) in each asymmetric unit. The two subunits, α and β , created by autocatalytic processing of uncleaved OAT2, do not correspond to separate domains. The α and β subunits remain tightly associated by non covalent bonds, with the whole of the α -subunit and the N-terminal part of the β -subunit forming a large domain with a smaller domain being made up of the remainder of the β -subunit.

In the apo-OAT2 structure,⁶⁴ the OAT2 molecules are packed such that the active site of one monomer is close to an intermolecular interface (Supporting Information, Figure 4). In contrast, in the acyl-OAT2 structure (2.1 Å), the four OAT2 monomers are arranged such that their active sites, including the C-terminal regions, are directed toward the solvent (Supporting Information, Figure 4). In contrast to the apo-OAT2 crystal structure, where only two out of the four protein chains showed electron density for the four C-terminal residues ($^{390}\text{EYTT}^{393}$), in the acyl-OAT2 structure, the complete C-terminus was resolved in all the chains and directed toward the active site. This observation suggests that the binding of a substrate (or intermediate) may stabilize the conformation of an otherwise mobile C-terminus.

Positive electron density was not observed around Thr-181 in molecule AB of the acyl-OAT2 structure. However, two additional regions of positive electron density were observed: one in the active site, and one close to the C-terminus. *N*- α -Acetyl-L-glutamate was too large to be refined into the additional regions of electron density, and glycerol and sulfate were too small. However, one molecule of Tris buffer, used for crystallization, refined well in to both regions of electron density.

Positive electron density was observed around γ -O of Thr-181 in three of the β -subunit chains (D, F, and H). Further rounds of refinement, retained the electron density around Thr-181. Refinement into the electron density was attempted with water, a Tris molecule and a sulfate ion but in each case the best fit was obtained with an acetyl group (Figure 3a). Sfcmap⁶⁵ and omitmap analyses⁶⁶ implied model bias was unlikely. For each of the acyl-enzyme complexes observed in the A, F, and H β -subunit chains continuous electron density was observed linking γ -O of Thr-181 with the assigned acetyl group. Although not possible to be certain at the 2.1 Å resolution of the analyses, the ester link of the acyl-enzyme complexes appears planar consistent with the conclusions arising from other crystallographic studies on acyl-enzyme complexes,^{26–28} including high-resolution studies on proteases.²⁷ The ester link is clearly in the thermodynamically preferred *Z* or (*cis*) geometry,⁶⁷ i.e., the methyl and methylene groups are in a *trans* arrangement, as observed in the crystal structures of other acyl-enzyme complexes derived from substrates.²⁶ The acyl-OAT2 structural data support the proposal that the *Z*-ester geometry is preferred under catalytic conditions. The carbonyl oxygen of acyl-Thr181 in chains D, F, and H is positioned similarly to be stabilized by the hydrogen bonding to the side-chain hydroxyl of Thr-111 (3.1 Å) and backbone amine of Gly-112 (2.9 Å) which were assigned as forming an oxyanion hole (Figure 3b and c). In each of the D, F, and H β -subunits chains, the side chain of Ser-219 was also found to be positioned to hydrogen bond to the O_γ of Thr-181; molecular dynamics simulations studies (see below) indicate that in solution a Ser-219 may hydrogen bond to the O_γ of Thr-181, so stabilizing the acyl-enzyme complex (Figure 3b and c). In the GH molecule, an acetate ion was refined close to the acyl-enzyme complex ester (Figure 3b and c).

(65) Vaguine, A. A.; Richelle, J.; Wodak, S. J. *Acta Crystallogr. D* **1999**, *55*, 191–205.

(66) Brünger, A. T.; Adams, P. D.; Clore, G. M.; DeLano, W. L.; Gros, P.; Grosse-Kunstleve, R. W.; Jiang, J.-S.; Kuszewski, J.; Nilges, M.; Pannu, N. S.; Read, R. J.; Rice, L. M.; Simonson, T.; Warren, G. L. *Acta Crystallogr. D* **1998**, *54*, 905–921.

(67) Deslongchamps, P. *Stereoelectronic Effects in Organic Chemistry*; Pergamon Press: New York, 1983; Chapter 3.

(62) Chaloner, P. A. J. *Perkin Trans.* **1980**, *2*, 1028–1035.

(63) Yoshida, N.; Yamasaki, M.; Ishii, S.-I. *J. Biochem.* **1973**, *1973*, 1175–1183.

(64) Elkins, J. M.; Kershaw, N. J.; Schofield, C. J. *Biochem. J.* **2005**, *385*, 565–573.

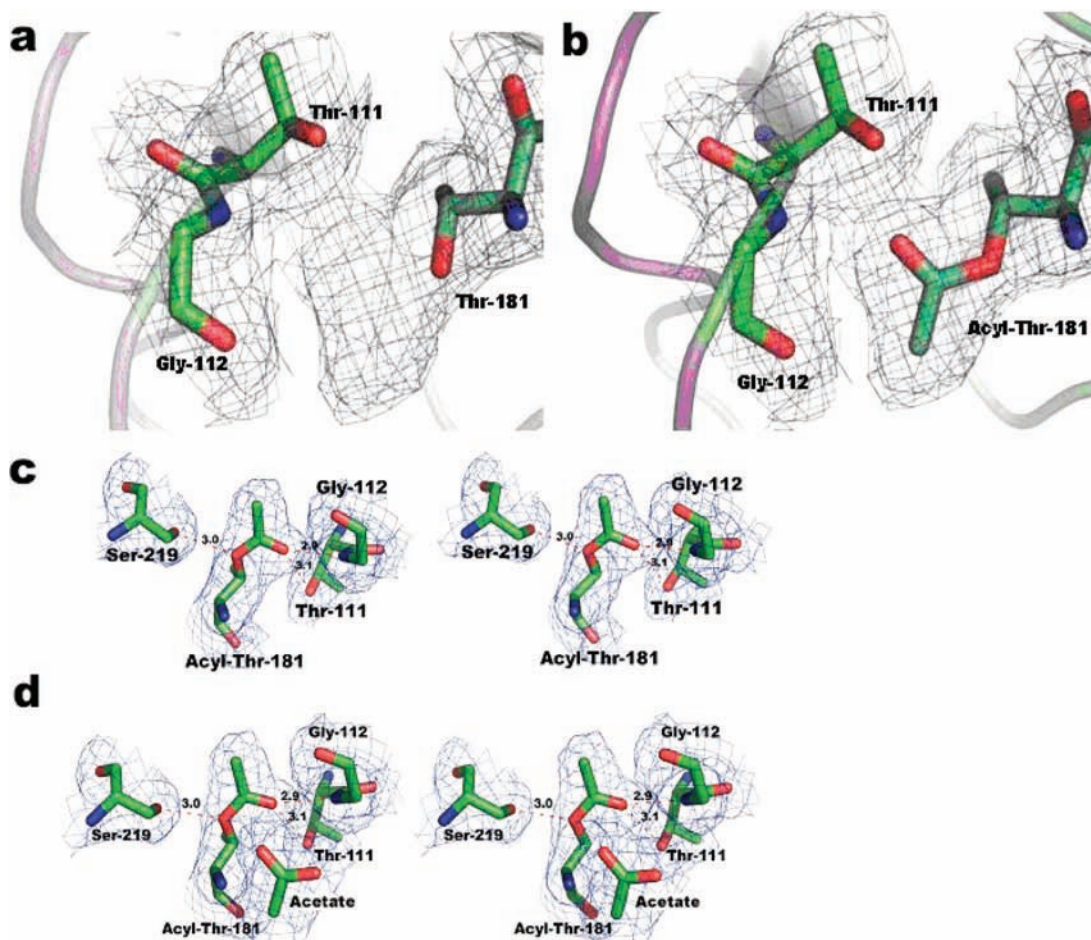


Figure 3. Views of the active site from an acyl-OAT2 crystal structure (CD molecule). The acetylated Thr-181 and the oxyanion hole residues Thr-111 and Gly-112 are shown. The 2mF_o-DF_c map in blue is contoured at 1 σ . (a) From a structural refinement without the acetyl group on Thr-181. (b) From a structural refinement with the acetyl group present. The pink map in both A and B is calculated by the SFCHECK⁶⁵ omit procedure. (c) Stereoview of the acyl-enzyme complex in molecule CD, showing interactions with oxyanion hole and Ser-219. The side-chain hydroxyl of Thr-111 and backbone amide of Gly-112 are positioned to stabilize the intermediate by hydrogen bonds to the carbonyl group oxygen (red dotted lines). (d) Stereoview of the acyl-enzyme complex in molecule GH in which an acyl-enzyme complex and an acetate ion have been refined. Ser-219 which is also positioned to stabilize the acyl-enzyme complex by interacting with the γ -O of Thr-181 is shown. The 2mF_o-DF_c maps for (c) and (d) are contoured to 1 σ .

IR Analyses. The crystallographic analyses revealed a single conformation for the acyl-enzyme complex of OAT2. However, IR studies on the acyl-enzyme complexes of a β -lactamase complex³² have revealed that more than one structure exists in solution where only one had been observed in a crystal structure. We therefore carried out IR analyses on the OAT2 acyl-enzyme complex. The kinetic analyses employing IR used OAT2 in which exchangeable hydrogens had been exchanged for deuterium, and a 10-fold excess of *N*- α -acetyl-L-glutamate. ¹³C and ¹²C versions of *N*- α -acetyl-L-glutamate were prepared to be used to enable isotope editing because substitution of ¹³C by ¹²C in a carbonyl group shifts the carbonyl stretch vibration to a lower frequency by ~ 38 cm⁻¹.⁶⁸ Subtraction of the equivalent ¹²C and ¹³C spectra gives a difference spectrum in which the acyl-enzyme complex can be isolated from the protein background.⁶⁸

The first acquisition, after all the necessary subtractions of the single turnover spectrum, indicated the presence of a broadband, from 1691 to 1710 cm⁻¹ (Supporting Information, Figure 5). This was assigned as an acyl-enzyme complex. The other observed features in the spectrum between 1660 and 1550 cm⁻¹ likely correspond to a slight imbalance in the ¹²C and ¹³C

experiments. Further kinetic analysis of the assigned acyl-enzyme complex band at 1691 cm⁻¹ showed that its intensity decreased with time, being observed for up to 45–60 min (half-life \approx 40 min); after this it was difficult to distinguish from the background (Supporting Information, Figure 6). Analysis by GEPASI⁶⁹ indicated the steady-state nature of the acyl-enzyme complex during the time course of analyses (up to 1702 s) (Supporting Information, Figure 6).

Close inspection of the broad acyl-enzyme complex band revealed it comprises two absorptions at 1691 and 1702 cm⁻¹, with the latter appearing as a shoulder on the former (Figure 4c). With repeated experiments the two absorbances (1691 and 1702 cm⁻¹) were always observed in the same ratio, suggesting that the complexes are in equilibrium. The total molar integrated intensity for the two bands at 1702 (73) and 1691 cm⁻¹ (50) of the acyl-enzyme complex was 123, by comparison with the integrated absorbance of a series of model esters, thus indicating $\sim 90\%$ acetylation which has previously been shown to be a reasonable assumption.³²

The 1660–1550 cm⁻¹ region in the difference IR spectrum (acyl-enzyme complex minus OAT2) corresponds to the amide-I and II region which represents protein conformational changes

(68) White, A. J.; Drabble, K.; Ward, S.; Wharton, C. W. *Biochem. J.* **1992**, *287*, 317–323.

(69) Mendes, P. *Trends Biochem. Sci.* **1997**, *22*, 361–363.

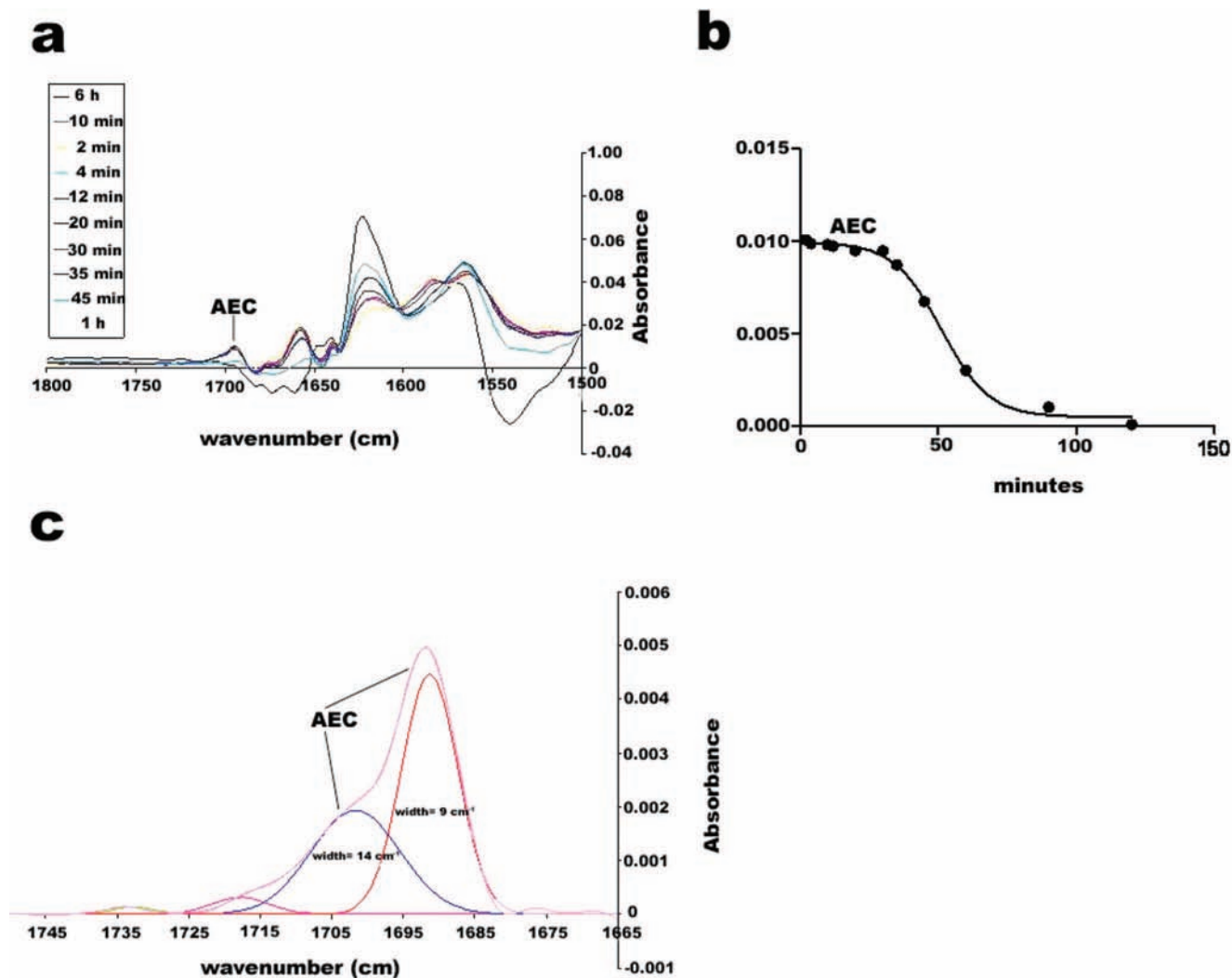


Figure 4. IR analyses of OAT2 catalysis. (a) IR time-course spectra from incubations of OAT2 with *N*- α -acetyl-L-glutamate showing the decrease in the presence of the absorption corresponding to the carbonyl of the acyl-enzyme intermediate ($1690\text{--}1710\text{ cm}^{-1}$, arrow) with time. Other features likely correspond to conformational changes and depletion of substrate during catalysis. (b) Kinetics of the hydrolysis of the OAT2 acyl-enzyme complex over time. (c) Difference IR spectra showing the two acyl-OAT2 absorptions. Band fitting with model esters reveals two major absorptions, with width (9 cm^{-1} , red) and (14 cm^{-1} , blue). The other two small absorptions at 1720 and 1734 cm^{-1} coincide with water vapor bands.

during catalysis. Analysis of this region in the difference spectrum (^{12}C and ^{13}C isotopic substitution) revealed negative inflection bands (Figure 5), indicating relaxation of OAT2 during catalysis upon acetylation.^{68,70}

Molecular Dynamics Simulations Studies. Because the IR results revealed two conformations for the acyl-enzyme complex, whereas the crystal structure implied only one conformation, we then carried out molecular dynamic simulations based on the crystallographic data to investigate the possibility of two equilibrating acyl-enzyme complexes.

Root mean square deviation (rmsd) analyses employing MD trajectories were carried out for the backbone $\text{C}\alpha$ atoms of an unmodified OAT2 monomer (AB molecule), an acyl-enzyme complex (CD molecule), and the acyl-enzyme complex in the presence of acetate (GH molecule) as reference structures. The average simulation rmsd values for the α -helices of the AB, CD, and GH molecules were 2.10 ± 0.13 (AB), 2.28 ± 0.19 (CD), and 1.94 ± 0.25 Å (GH) and 1.58 ± 0.15 (AB), 1.69 ± 0.28 (CD), and 1.88 ± 0.45 Å (GH) for the β -sheets. Supporting

Information, Figure 7 shows the rmsd of the secondary structural features of acyl-OAT2 over a simulation of 4 ns. It is evident from the results that very minor deviations were observed from the unmodified structure ($1\text{--}2$ Å), suggesting that no major ‘global’ structural reorganization occurs upon acyl-enzyme complex formation.

At some time points in the molecular dynamics simulations on the CD and GH monomers of the acyl-OAT2 structure, it was observed that the Thr-111 hydroxyl hydrogen ‘flipped’ away from the oxyanion hole, resulting in the loss of a hydrogen bond to the acyl-enzyme complex carbonyl oxygen. After flipping, the Thr-111 side chain was observed to hydrogen bond with the backbone carbonyl of acetylated Thr-181 (Figure 5). In summary, three significant hydrogen-bonding conformations for the oxyanion hole involving residues were observed. (i) The longest lived structure in which the acyl-enzyme complex is positioned to make hydrogen bonds with both Thr-111 and Gly-112 ($t = 1.0$ ns in Figure 5b), (ii) a less stable structure in which the acyl-enzyme complex is positioned to make hydrogen bonds with only Gly-112 ($t = 0$ and 6.3 ns in Figure 5b), and (iii) a very transient structure in which the acyl-enzyme complex did

(70) Barth, A.; Zscherp, C. *Q. Rev. Biophys.* **2002**, *35*, 369–430.

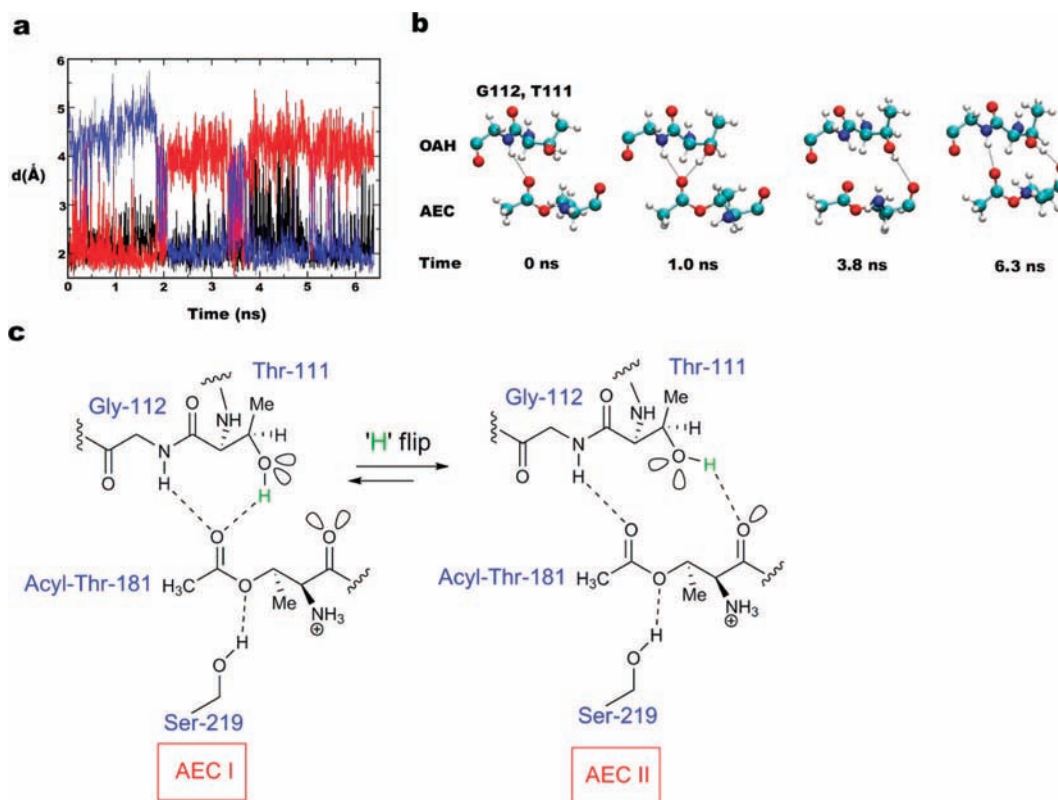


Figure 5. Molecular dynamics simulations of the OAT2 acyl-enzyme complex showing hydrogen bonding of the acyl-enzyme with Thr-111 and Gly-112. (a) Distances (Å) between the side chain hydroxyl hydrogen of Thr-111 and the acyl-enzyme complex carbonyl oxygen (red) and between the backbone amide of Gly-112 (black) versus molecular dynamics simulations time. The blue plot corresponds to the distance between the hydroxyl hydrogen of Thr-111 and backbone carbonyl oxygen of Thr-181. (b) Conformations of the acyl-enzyme complex at selected time points (see text for discussion). Note the loss of one of the oxyanion hole hydrogen bonds (to Thr-111) is shown at 6.3 ns. The conformation shown at 1.0 ns dominated during the molecular dynamics simulations (4.2/6.3 ns). We propose that this conformation corresponds to the IR band at 1690 cm^{-1} . (c) Schematic illustrating the ‘H-flip’ of Thr-111 side-chain alcohol, resulting in the second acyl-enzyme complex structure. The lone pair orbitals on selected oxygens are shown.

not make hydrogen bonds with Thr-111 and Gly-112 ($t = 3.8$ ns in Figure 5b).

Conclusions

The combined biophysical analyses demonstrate that OAT2 catalysis proceeds via an acyl-enzyme complex. MS studies, on intact protein and following trypsin digestion, provide direct evidence for the proposal that Thr-181 located at the N-terminus of the OAT2 β -subunit acts as the nucleophilic residue in OAT2 catalysis.^{45,64} ^{13}C NMR analyses, using ^{13}C - N - α -acetyl-L-glutamate, supported the presence of an acyl-enzyme complex in solution, with an assigned resonance at 176.9 ppm; this value is similar to that reported for acyl-enzyme complexes formed by the reaction of α -chymotrypsin and p -nitrophenyl acetate substrate analogues (174 ppm, pH 3;⁶¹ and 176.5 ppm, pH 3, $-20\text{ }^\circ\text{C}$, low pH was used to stabilize the acyl-enzyme complexes⁷¹), and for nucleophilic enzymes catalyzing C–C bond cleavage (170 ppm).⁷² Significantly, we observed the OAT2 acyl-enzyme complex to have a much longer half-life (~ 40 min) than reported for acyl-enzyme complexes in protease catalysis (e.g., the half-life of a α -chymotrypsin acyl-enzyme complex with p -nitrophenyl acetate substrate analogue was reported to be 2 min at pH 8).⁶¹

The relatively long half-life of the OAT2 acyl-enzyme complex encouraged us to carry out crystallographic analyses under catalytically active conditions. In the presence of an excess of an acetylated substrate (N - α -acetyl-L-glutamate), the results revealed that the alcohol of Thr-181 was indeed acetylated in the acyl-enzyme complex, and that the acyl-enzyme complex carbonyl is located in an oxyanion hole, formed by the backbone/amide NH of Gly-112 and the alcohol side chain of Thr-111. Whereas in most serine/cysteine proteases, the oxyanion hole is formed by two backbone amide NH groups,^{13,14,29} there is precedent for variations, e.g., in prolyl oligopeptidase where the side chain hydroxyl of Tyr473 is the other oxyanion hole component apart from the backbone amide of Ser554.⁷³ Molecular dynamics simulations studies on OAT2 acyl-enzyme complex revealed that a second hydrogen bonding interaction to the acyl-enzyme complex may occur, because the side chain of Ser-219 is close to O_γ of Thr-181 (3.0 Å); this interaction may contribute to the long lifetime of the OAT2 acyl-enzyme complex.

Previous IR studies on acyl-enzyme complexes of nucleophilic enzymes with inhibitors have shown that, whereas crystallographic analyses may imply only a single structure, in solution several acyl-enzyme complex conformations can occur.^{32–34} Flow-quenched IR studies on OAT2 led to the observation of a broadband at $\sim 1691\text{--}1702\text{ cm}^{-1}$, assigned as an acyl-enzyme complex. The half-life of the band was very

(71) Mackenzie, N. E.; Malthouse, J. P.; Scott, A. I. *Biochem. J.* **1984**, *219*, 437–444.

(72) Li, J. J.; Li, C.; Blindauer, C. A.; Bugg, T. D. *Biochemistry* **2006**, *45*, 12461–12469.

(73) Sztelnner, Z.; Renner, V.; Polgár, L. *Protein Sci.*, **9**, 353–360.

similar (45 min) to the resonance assigned to three acyl-enzyme complex by ^{13}C NMR (40 min). Close analysis of the broadband observed in the IR revealed that it is comprised of two bands, one at 1691 cm^{-1} and one at 1702 cm^{-1} . We propose that the band at 1691 cm^{-1} corresponds to an acyl-enzyme complex structure in which the amide carbonyl forms two hydrogen bonds in the oxy-anion hole. The band at 1702 cm^{-1} is proposed to be a singly hydrogen-bonded species that was not observed in the crystallographic studies. Molecular dynamics simulations supported these proposals; in these studies at some time points the hydroxyl hydrogen of Thr-111 was observed to 'flip' away from the oxyanion hole, to hydrogen bond with the backbone carbonyl of Thr-181; this arrangement is proposed to correspond to the IR band at 1702 cm^{-1} .

Precedent for the observation of more than one acyl-enzyme complex structure in solution comes from the work on the complex formed between serine β -lactamase and methicillin. In the case of the acyl-enzyme complex formed with this β -lactamase and aztreonam (a poor substrate/inhibitor),³² four IR bands, at 1746 , 1727 , 1708 , and 1691 cm^{-1} , were observed. In contrast to the 'hydrogen-flip' we propose to be responsible for the interconversion of the two OAT2 acyl-enzyme complex structures, in the β -lactamase, molecular dynamics simulations indicate that the acyl-enzyme complex carbonyl group can move out of the oxyanion hole to hydrogen bond to the side chain of Tyr-221 to give a second acyl-enzyme complex structure.³² Very recently the crystal structure of the β -lactamase SHV-1 complexed with Meropenem revealed two conformations of the acyl-enzyme complex: one where the Meropenem carbonyl oxygen was located in the oxyanion hole and a second in which it was not.³⁵

A further difference between the OAT2 and β -lactamase work is in apparent changes observed by IR corresponding to the secondary structure. In the β -lactamase work, upon acylation changes in the spectrum were associated with tightening of the β -sheets around the active site. In the case of OAT2 the IR data suggest an apparent relaxation of the overall structure. The available crystallographic data are consistent with this proposal because the active site in the acyl-OAT2 structure is more open to the solvent than in the modified OAT2 structure,⁴⁵ possibly

in order to enable L-glutamate/L-ornithine to bind at the active site. It is also possible that the C-terminal region, which was unresolved in the unmodified OAT2 structure but resolved in the acyl-OAT2 structure, may be involved in substrate binding.

Overall, the results have provided detailed insights into the acyl-enzyme complex structure of OAT2 under catalytically relevant conditions. The conclusion that the acyl-enzyme complex adopts at least two distinct structures, as revealed by IR (but not by other biophysical analyses), suggests that a re-evaluation of the solution structures of acyl-enzyme complexes of other nucleophilic enzymes is of interest. Given that a widely used approach in the inhibition of nucleophilic enzymes involves the formation of stable acyl-enzyme complexes, a rational approach to the optimization of such inhibitors may best employ combined biophysical analyses in both the crystalline and solution states.

Acknowledgment. We gratefully acknowledge Rasheduzzaman Chowdhury, Tom Walter, and Oxford Protein Production Facility for assistance with crystallization of OAT2. Thanks to Jasmin Mecinovic with the help in synthesis of ^{13}C -*N*-acetyl-L-glutamate and Kanjana Thumanu for her help with the initial IR experiments with OAT2. C.D. thanks the Royal Society for a University Research Fellowship. We thank OSC for providing computational resources.

Supporting Information Available: The refinement statistics of the OAT2 acyl-enzyme crystal structure, observation of the ^{13}C -acyl-enzyme complex by NMR and IR, ^{13}C NMR experiments with α -chymotrypsin and phenylpropionic acid, overall view of the OAT2 acyl-enzyme crystal structure showing all four molecules, crystal structure snapshots of the OAT2 acyl-enzyme active site interface and comparison with the wild-type structure, kinetics of the OAT2 acyl-enzyme hydrolysis by IR using GEPASI, and rmsd of the secondary structural features of acyl-OAT2 over a simulation of 4 ns. This material is available free of charge via the Internet at <http://pubs.acs.org>.

JA807215U